IUCrJ

Volume 11 (2024)

**Supporting information for article:**

# Conformation-aggregation interplay in the simplest aliphatic ethers probed under high pressure

Natalia Sacharczuk, Anna Olejniczak, Maciej Bujak, Kamil Filip Dziubek, Andrzej Katrusiak and Marcin Podsiadło

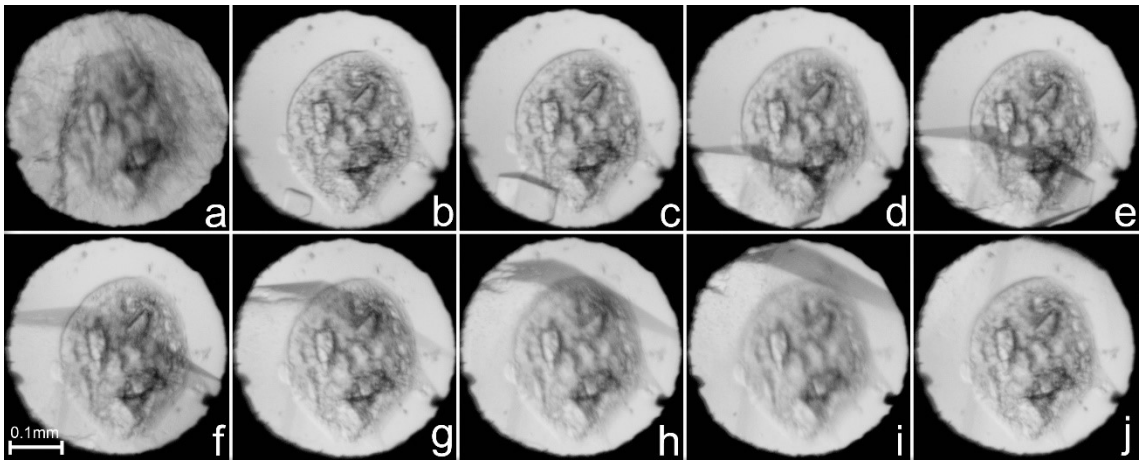


**Figure S1.** Stages of the dimethyl ether (DME) phase β single-crystal growth inside the DAC chamber: (a) polycrystalline mass grown isothermally at 295 K; (b) one crystal seed at 325 K; (c-i) the single crystal cooled to 311 K and (j) filling the whole volume of the DAC chamber at 295 K and 3.30 GPa. The ruby chips, for pressure calibration, lie in the central part of the DAC.

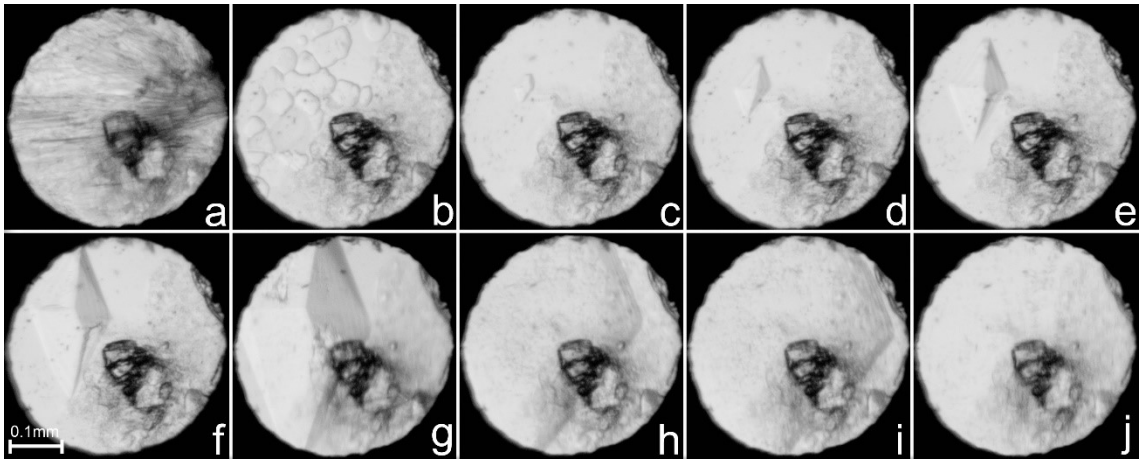


**Figure S2.** Stages of the DME phase β single-crystal growth inside the DAC chamber: (a) polycrystalline mass grown isothermally at 295 K; (b) polycrystal–liquid equilibrium at 351 K; (c) one crystal seed at 353 K; (d-i) the single crystal cooled to 347 K and (j) filling the DAC chamber at 295 K and 3.90 GPa. The ruby chip, for pressure calibration, is located in the central part of the DAC.

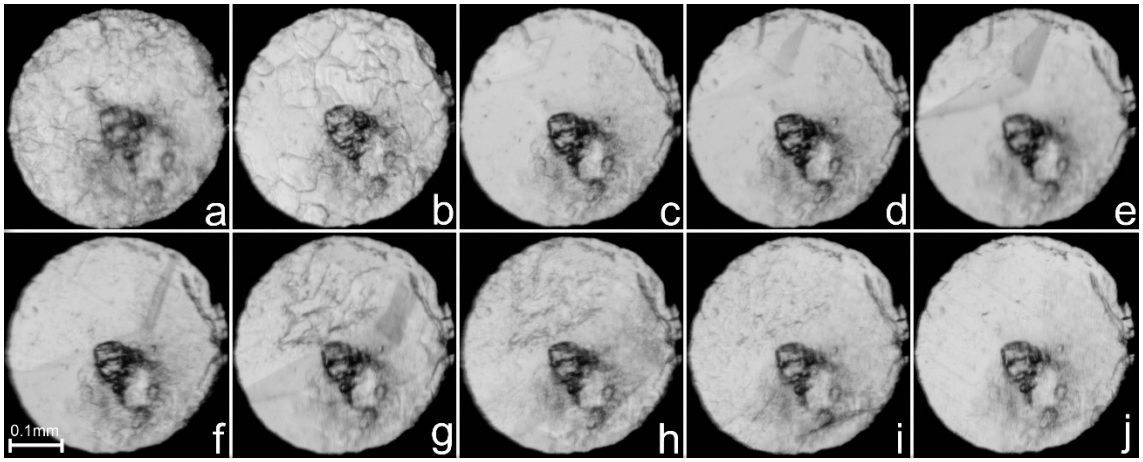


**Figure S3.** Stages of the DME phase β single-crystal growth inside the DAC chamber: (a) polycrystalline mass grown isothermally at 295 K; (b) polycrystal–liquid equilibrium at 360 K; (c) one crystal seed at 361 K; (d-i) the single crystal cooled to 346 K and (j) filling the whole volume of the DAC chamber at 295 K and 4.30 GPa. The ruby chip, for pressure calibration, is placed in the central part of the DAC.

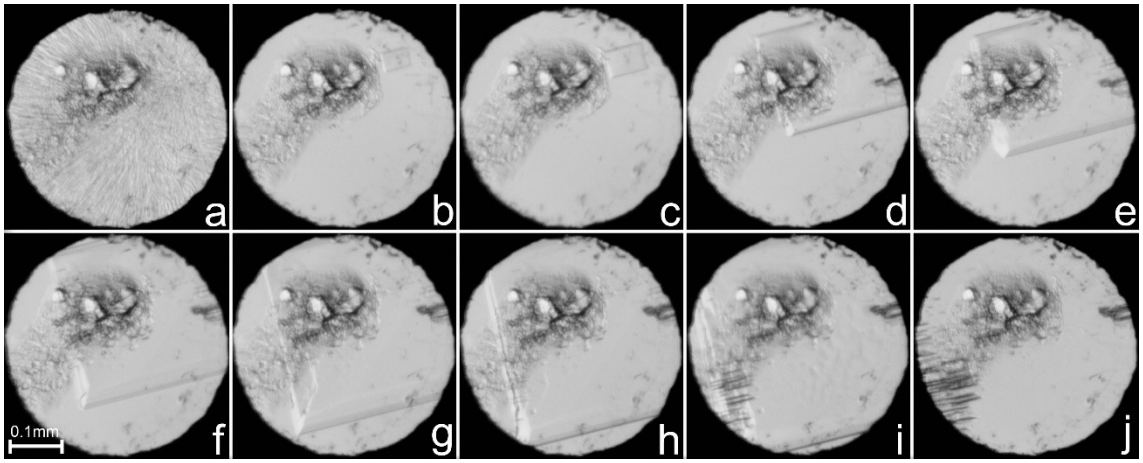


**Figure S4.** Stages of the DME phase γ single-crystal growth inside the DAC chamber: (a) polycrystal mass grown isothermally at 295 K; (b) one crystal seed at 361 K; (c-i) the single crystal cooled to 351 K and (j) filling the DAC chamber at 295 K and 4.50 GPa. The ruby chips, for pressure calibration, lie in the upper part of the DAC.

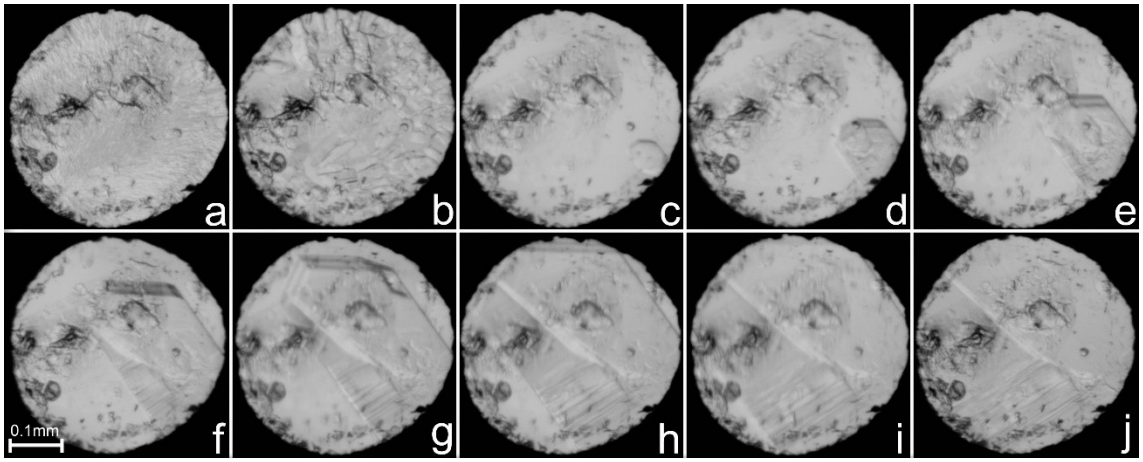


**Figure S5.** Stages of the DME phase γ single-crystal growth inside the DAC chamber: (a) polycrystalline mass grown isothermally at 295 K; (b) polycrystal–liquid equilibrium at 372 K; (c) one crystal seed at 374 K; (d-i) the single crystal cooled to 369 K and (j) filling the whole volume DAC chamber at 295 K and 5.60 GPa. The ruby chips, for pressure calibration, are placed in the central and left part of the DAC.

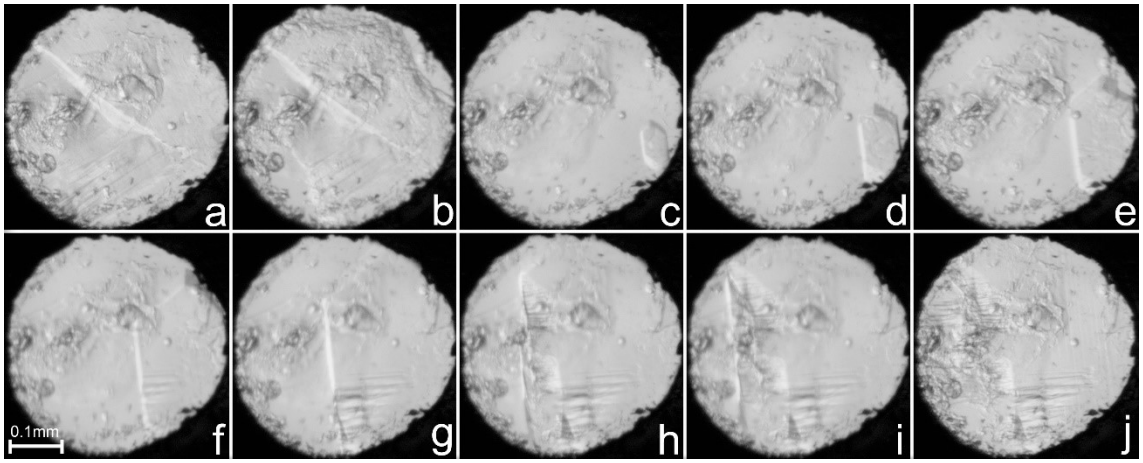


**Figure S6.** Stages of the DME phase γ single-crystal growth inside the DAC chamber: (a) polycrystalline mass grown isothermally at 295 K; (b) polycrystal–liquid equilibrium at 396 K; (c) one crystal seed at 399 K; (d-i) the single crystal cooled to 394 K and (j) filling the whole volume DAC chamber at 295 K and 7.30 GPa. The ruby chips, for pressure calibration, lie in the central and left part of the DAC.

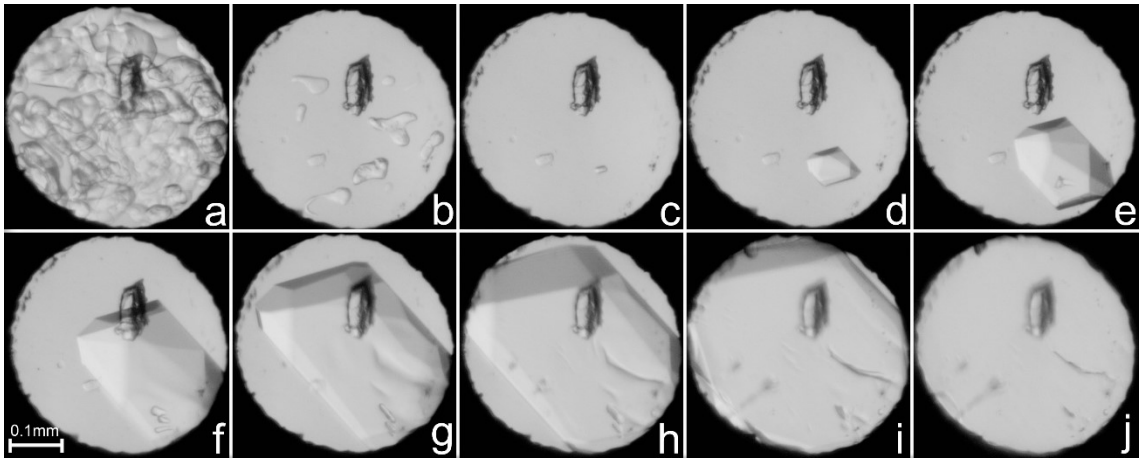


**Figure S7.** Stages of the diethyl ether (DEE) phase β single-crystal growth inside the DAC chamber: (a) polycrystalline mass grown isothermally at 295 K; (b) polycrystal–liquid equilibrium at 344 K; (c) one crystal seed at 345 K; (d-i) the single crystal cooled to 317 K and (j) filling the whole volume of DAC chamber at 295 K and 1.85 GPa. The ruby chip, for pressure calibration, is placed in the central part of the DAC chamber.

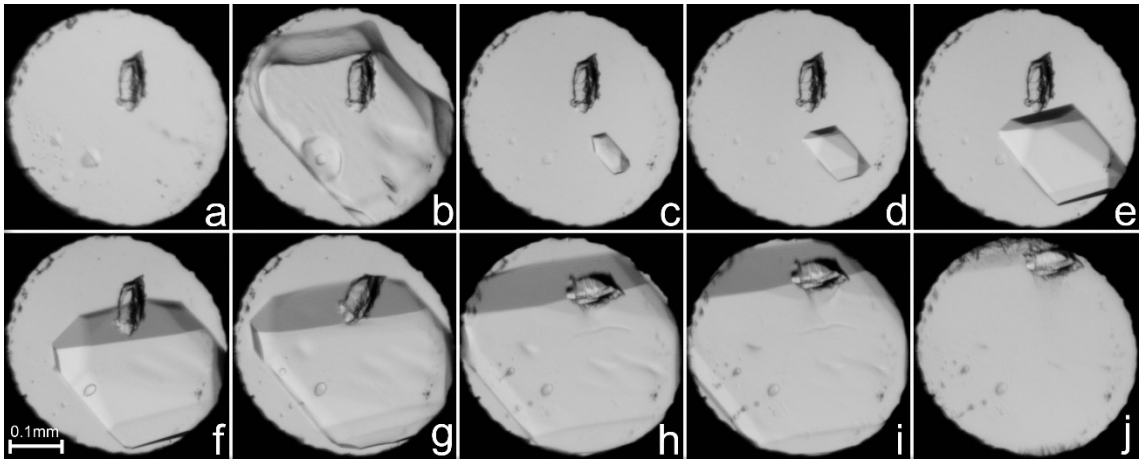


**Figure S8.** Stages of the DEE phase β single-crystal growth inside the DAC chamber: (a) single-crystal–liquid equilibrium at 308 K; (b) single-crystal–liquid equilibrium at 348 K; (c) one crystal seed at 352 K; (d-i) the single crystal cooled to 331 K and (j) filling the DAC chamber at 295 K and 2.15 GPa. The ruby chip, for pressure calibration, lie in the central part (a-f) and then it is moved to the upper part (g-j) of the DAC.

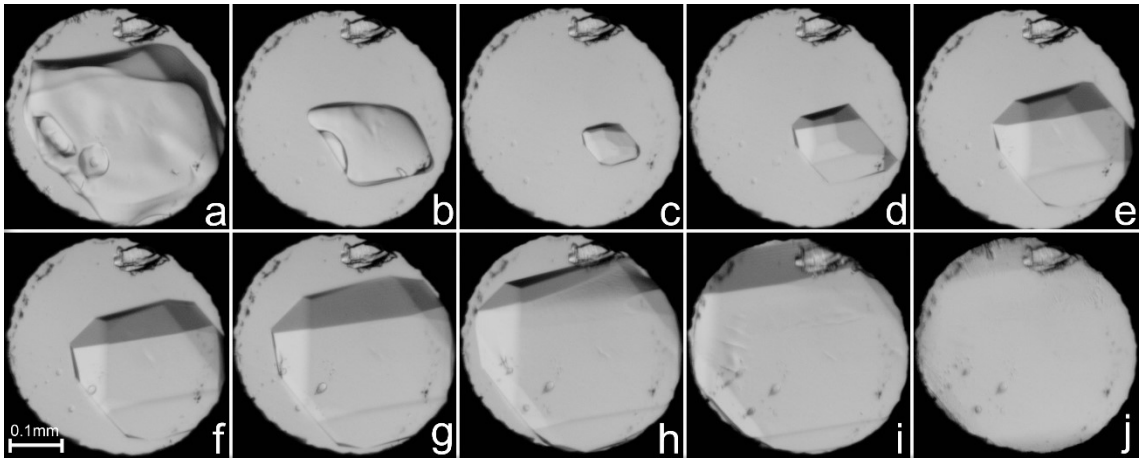


**Figure S9.** Stages of the DEE phase β single-crystal growth inside the DAC chamber: (a) single-crystal–liquid equilibrium at 360 K; (b) single-crystal–liquid equilibrium at 361 K; (c) one crystal seed at 362 K; (d-i) the single crystal cooled to 338 K and (j) filling the whole volume of DAC chamber at 295 K and 2.45 GPa. The ruby chip for pressure calibration is located in the upper part of the DAC.

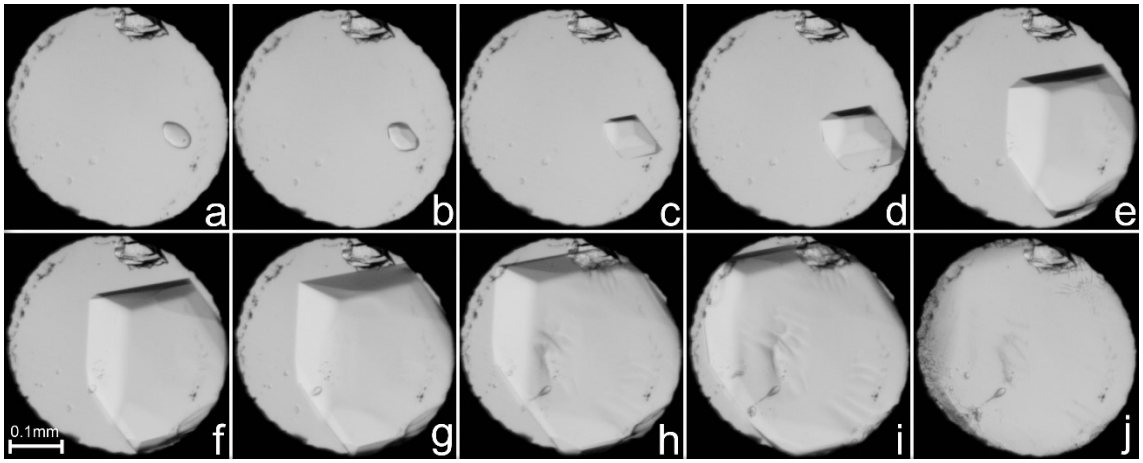


**Figure S10.** Stages of the DEE phase β single-crystal growth inside the DAC chamber: (a) one crystal seed at 368 K; (b-i) the single crystal cooled to 345 K and (j) filling the DAC chamber at 295 K and 2.65 GPa. The ruby chip, for pressure calibration, lies in the upper part of the DAC.

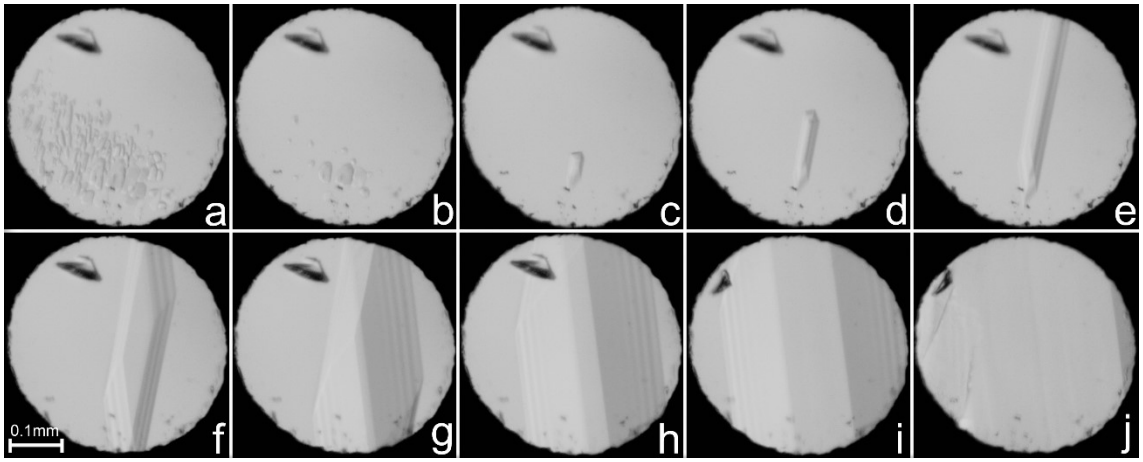


**Figure S11.** Stages of the DEE phase γ single-crystal growth inside the DAC chamber: (a) polycrystal–liquid equilibrium at 361 K; (b) polycrystal–liquid equilibrium at 363 K; (c) one crystal seed at 359 K; (d-i) the single crystal cooled to 331 K and (j) filling the whole volume of DAC chamber at 295 K and 2.65 GPa. The ruby chip, for pressure calibration, lies in the upper part of the DAC.

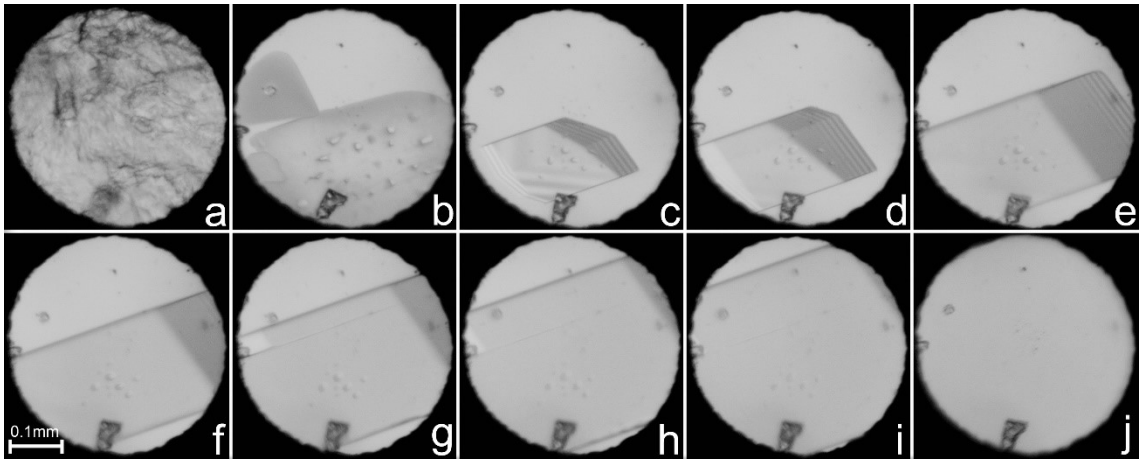


**Figure S12.** Stages of the DEE phase δ single-crystal growth inside the DAC chamber: (a) polycrystalline mass grown isothermally at 295 K; (b) three single-crystals–liquid equilibrium at 405 K; (c) one crystal seed at 391 K; (d-i) the single crystal cooled to 341 K and (j) filling the DAC chamber at 295 K and 2.80 GPa. The ruby chip, for pressure calibration, lies in the bottom part of the DAC.

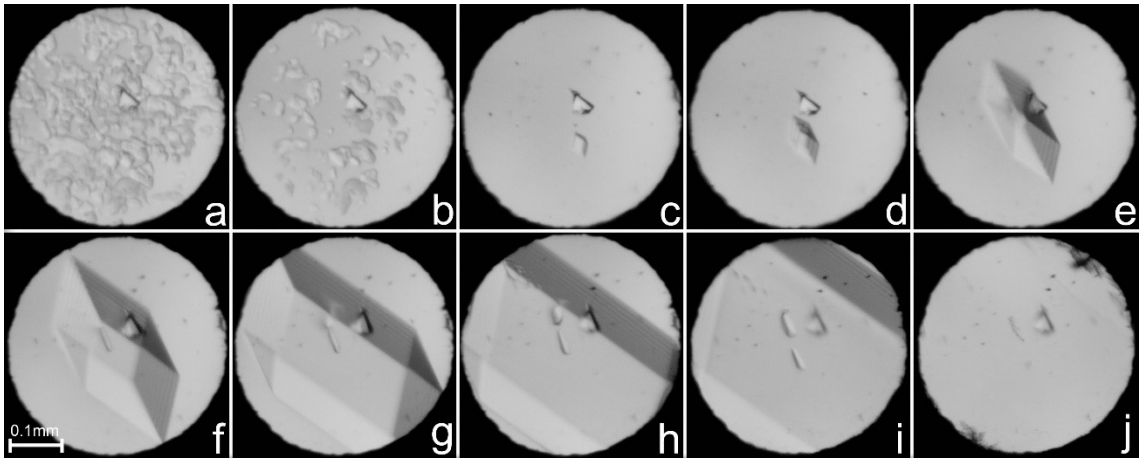


**Figure S13.** Stages of the DEE phase δ single-crystal growth inside the DAC chamber: (a) polycrystal–liquid equilibrium at 443 K; (b) polycrystal–liquid equilibrium at 444 K; (c) one crystal seed at 445 K; (d-i) the single crystal cooled to 387 K and (j) filling the whole volume of DAC chamber at 295 K and 3.45 GPa. The ruby chip, for pressure calibration, lies in the central part of the DAC.

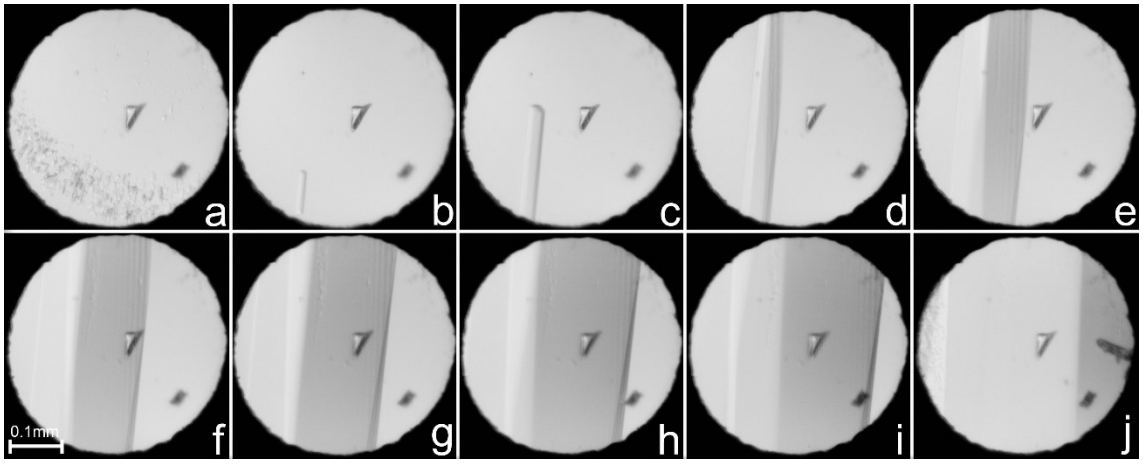


**Figure S14.** Stages of the dipropyl ether (DPE) phase α single-crystal growth inside the DAC chamber: (a) polycrystal–liquid equilibrium at 334 K; (b) one crystal seed at 334 K; (c-i) the single crystal cooled to 306 K and (j) filling the DAC chamber at 295 K and 1.70 GPa. The ruby chip, for pressure calibration, lies in the central part of the DAC.

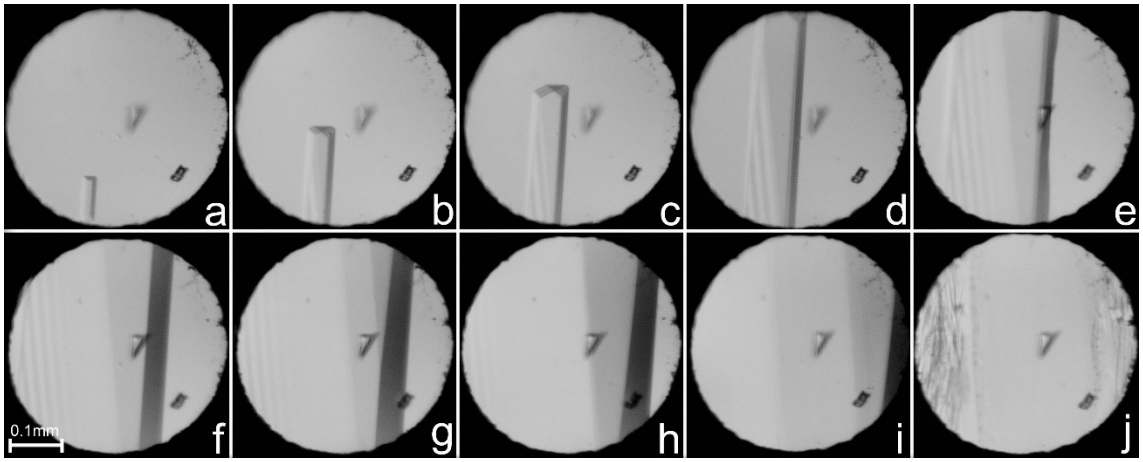


**Figure S15.** Stages of the DPE phase α single-crystal growth inside the DAC chamber: (a) one crystal seed at 356 K; (b-i) the single crystal cooled to 318 K and (j) filling the whole volume of DAC chamber at 295 K and 2.10 GPa. The ruby chip, for pressure calibration, lies in the central part of the DAC.

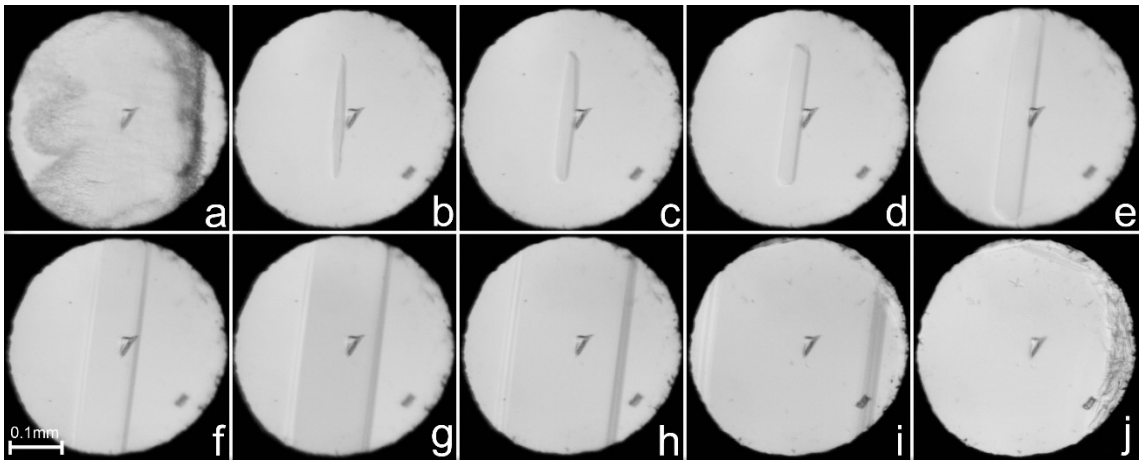


**Figure S16.** Stages of the DPE phase α single-crystal growth inside the DAC chamber: (a) polycrystal–liquid equilibrium at 393 K; (b) one crystal seed at 396 K; (c-i) the single crystal cooled to 356 K and (j) filling the DAC chamber at 295 K and 2.80 GPa. The ruby chip for pressure calibration lies in the central part of the DAC.

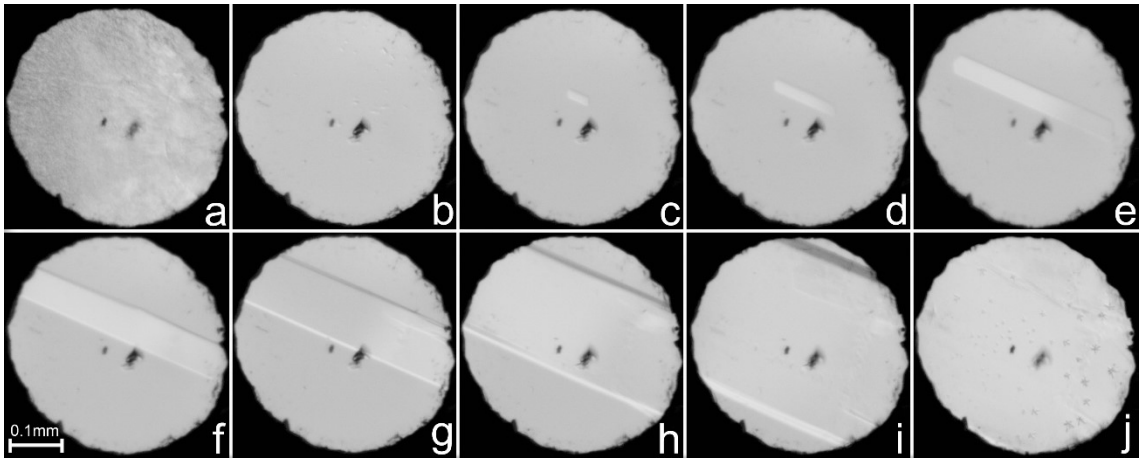


**Figure S17.** Stages of the DPE phase α single-crystal growth inside the DAC chamber: (a) polycrystal–liquid equilibrium at 295 K; (b) polycrystal–liquid equilibrium at 437 K; (c) one crystal seed at 433 K; (d-i) the single crystal cooled to 401 K and (j) filling the whole volume of DAC chamber at 295 K and 3.85 GPa. The ruby chip, for pressure calibration, lies in the central part of the DAC.

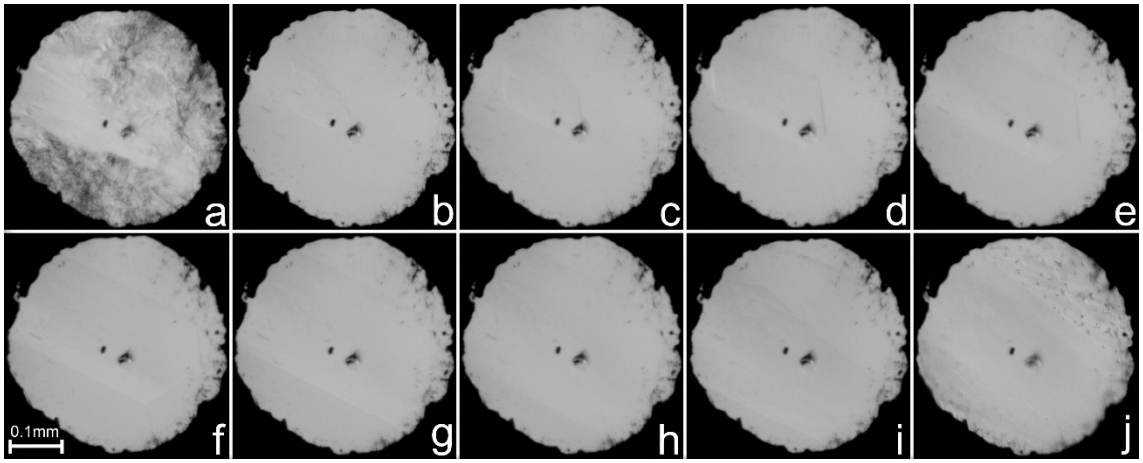


**Figure S18.** Stages of the DPE phase α single-crystal growth inside the DAC chamber: (a) polycrystal–liquid equilibrium at 295 K; (b) one crystal seed at 483 K; (c-i) the single crystal cooled to 424 K and (j) filling the DAC chamber at 295 K and 5.30 GPa. The ruby chip, for pressure calibration, lies in the central part of the DAC.

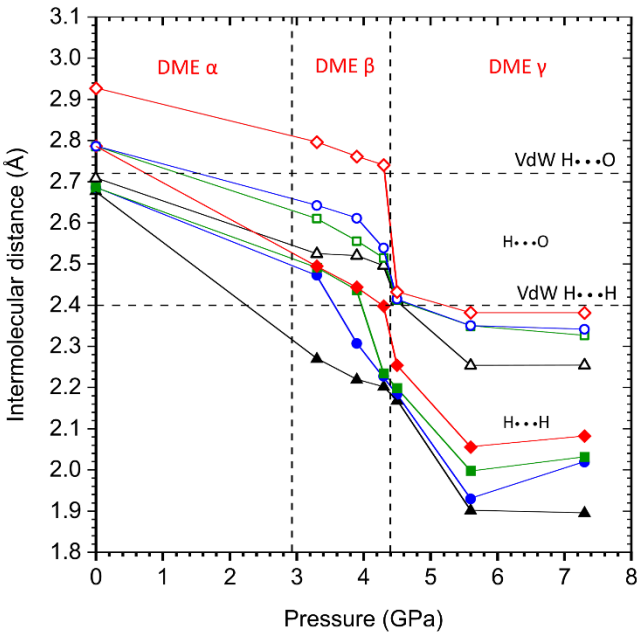


**Figure S19.** Intermolecular distances plotted as a function of pressure in DME. Four shortest distances for two types of interactions are presented: full shapes represent H···H whereas empty shapes depict the H···O distances. The black horizontal lines show the sum of the van der Waals radii of H and O of 2.72 Å, of H and H of 2.4 Å. The estimated standard deviations are smaller than the plotted symbols.

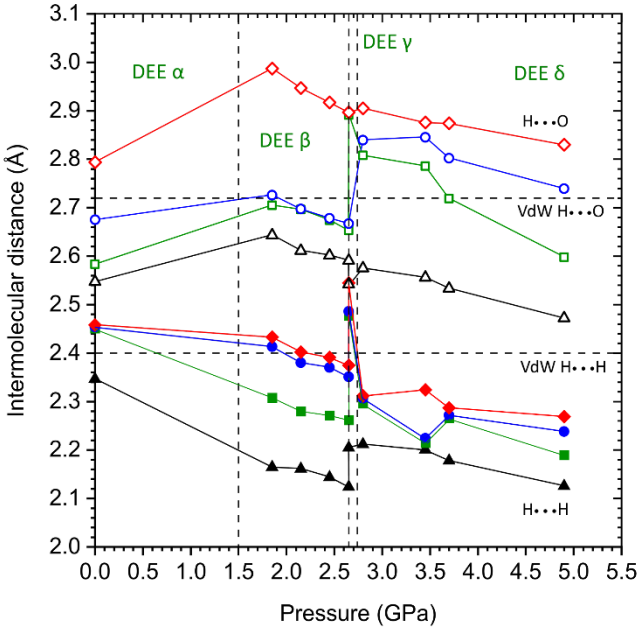


**Figure S20.** Intermolecular distances plotted as a function of pressure in DEE. Four shortest distances for two types of interactions are presented: full shapes represent H···H whereas empty shapes depict the H···O distances (only two shortest H···O distances for DEE γ are indicated). The black horizontal lines show the sum of the van der Waals radii of H and O of 2.72 Å, and of H and H of 2.4 Å. The estimated standard deviations are smaller than the plotted symbols.

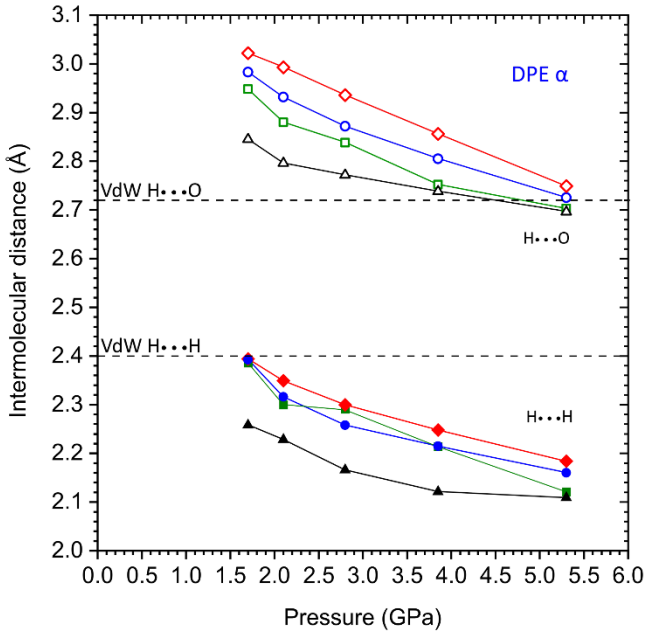


**Figure S21.** Intermolecular distances plotted as a function of pressure in DPE. Four shortest distances for two types of interactions are presented: full shapes represent H···H whereas empty shapes depict the H···O distances. The black horizontal lines show the sum of the van der Waals radii of H and O of 2.72 Å, and of H and H of 2.4 Å. The estimated standard deviations are smaller than the plotted symbols.

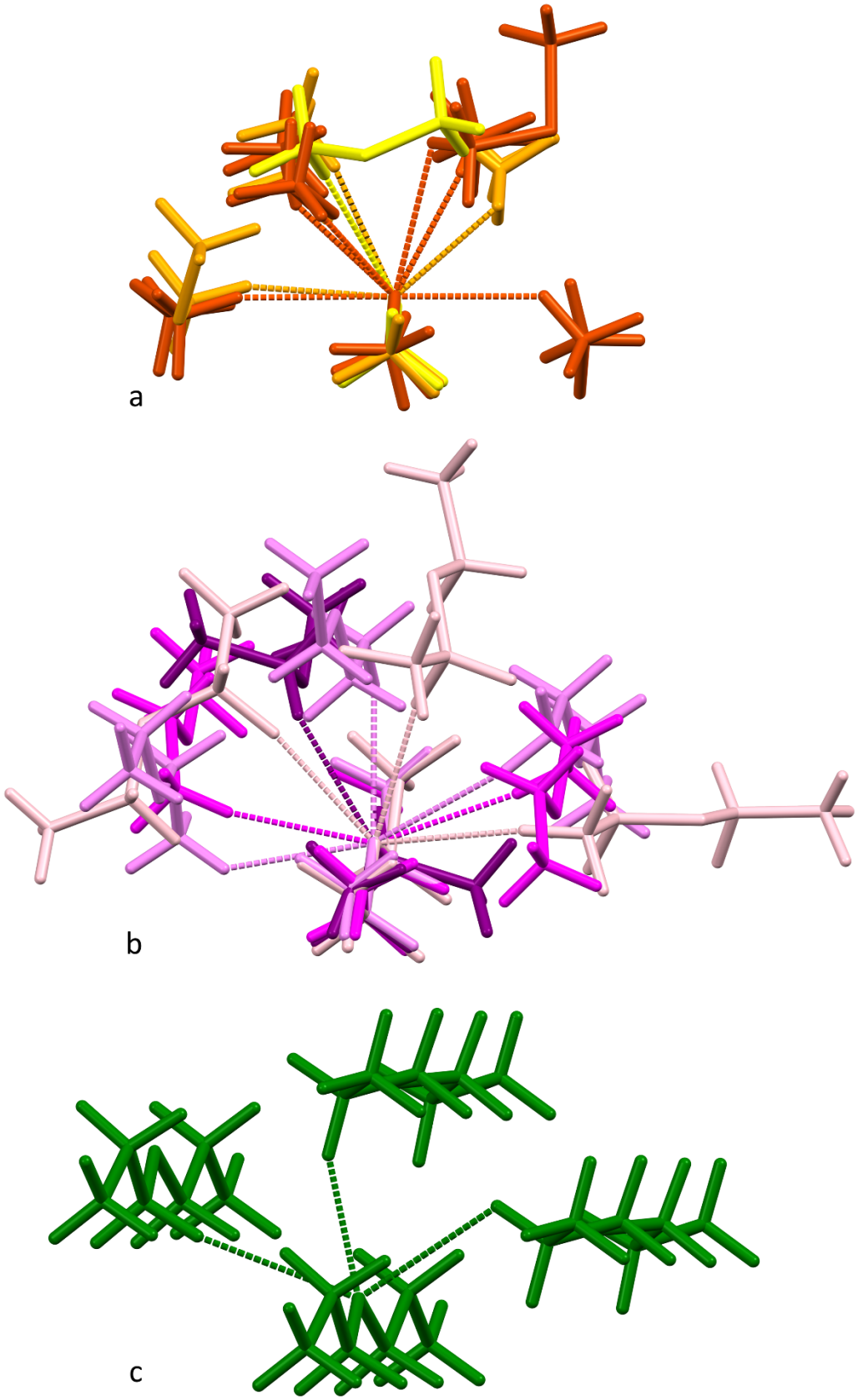


**Figure S22.** The shortest intermolecular CH···O interactions in: (a) DME phases α (yellow), β (orange) and γ (brown); (b) DEE phases α (pink), β (violet), γ (magenta) and δ (purple) and (c) DPE phase α (green).

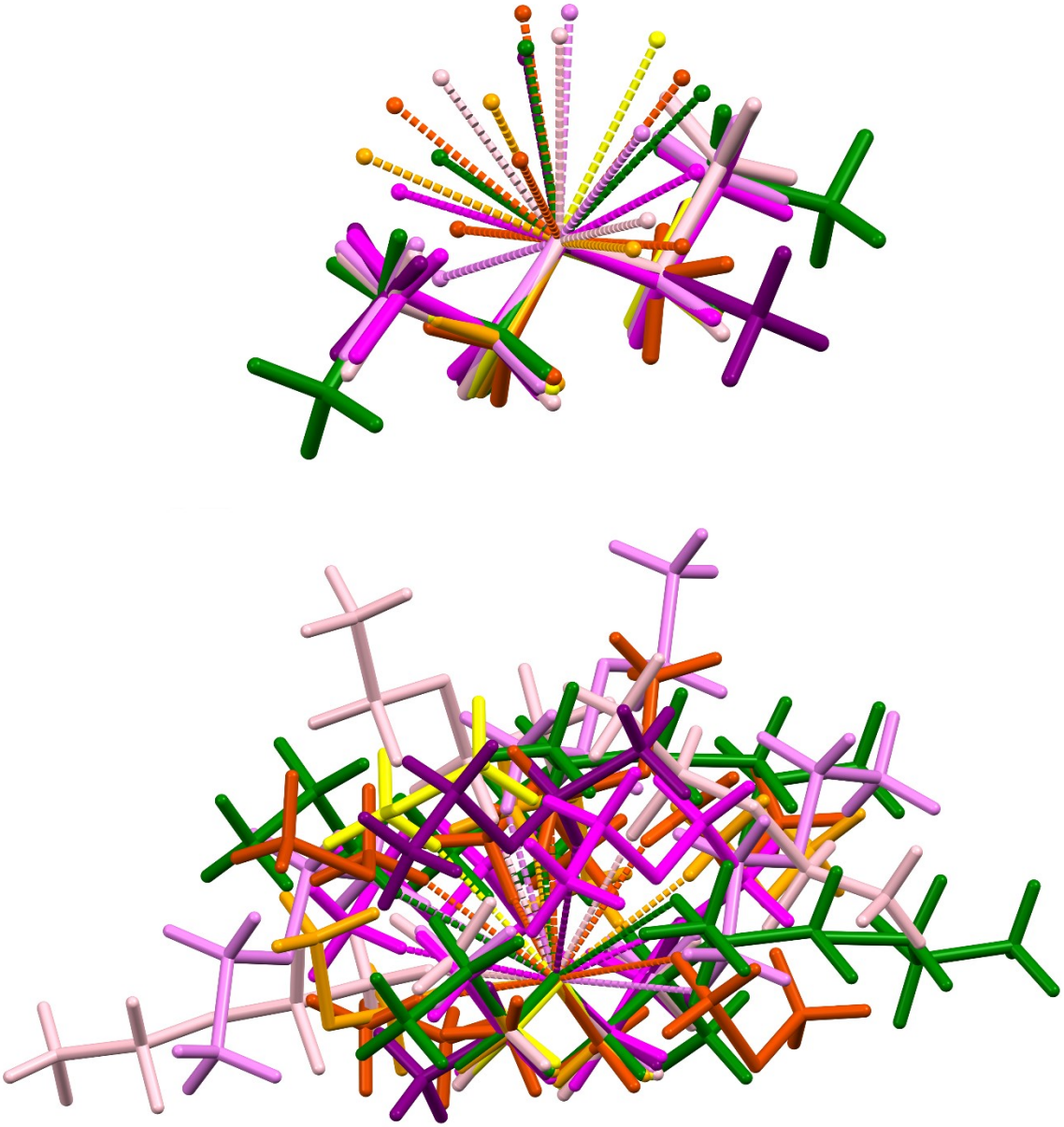

**Figure S23.** The shortest intermolecular CH···O interactions in the superimposed molecules of DME: phases α (yellow), β (orange), γ (brown); DEE phases α (pink), β (violet), γ (magenta), δ (purple) and DPE phase α (green) (*cf*. Fig. 5).

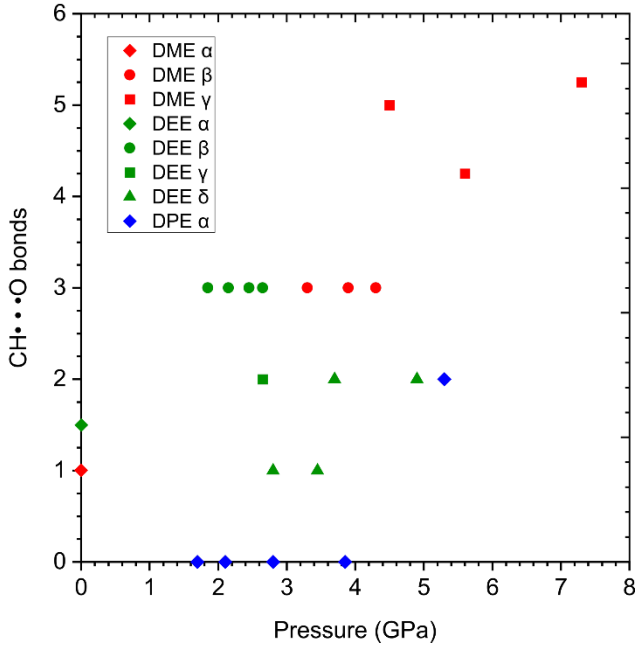


**Figure S24.** The number of H-donors accepting the O-atoms within the hydrogen bonds CH···O (per one molecule in the unit cell) in different phases of DME, DEE and DPE.

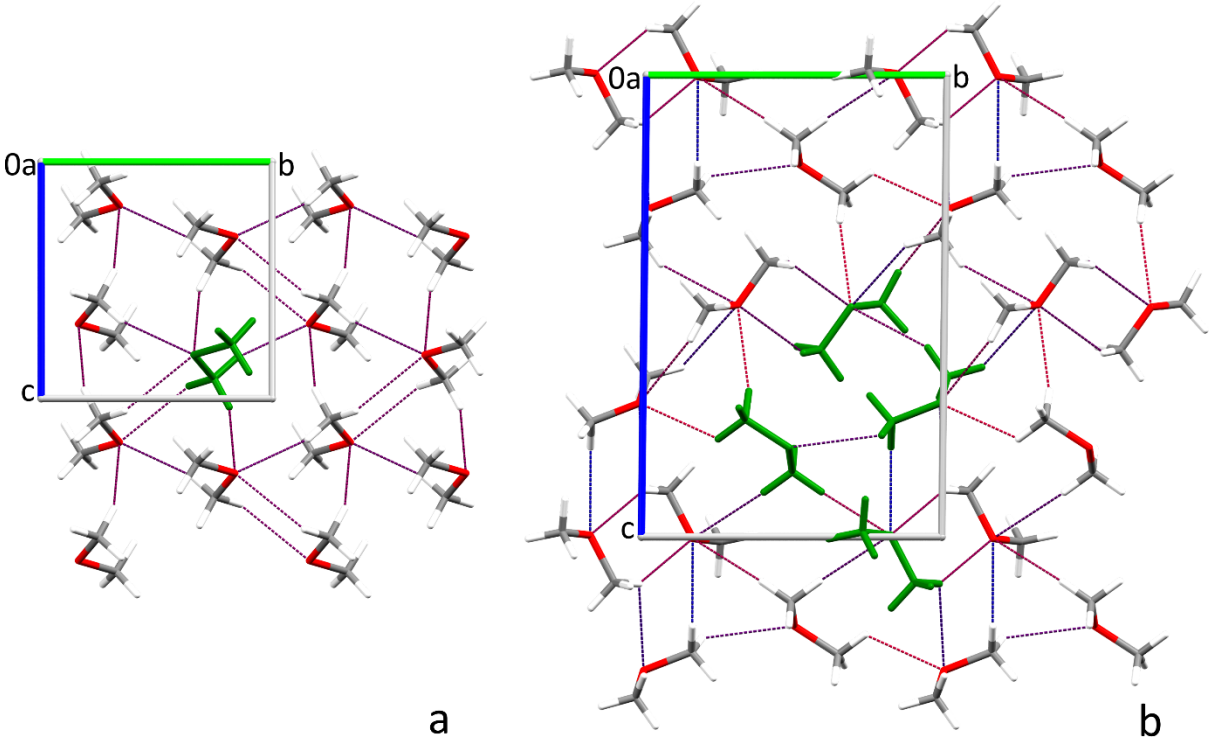


**Figure S25.** CH···O hydrogen bonding patterns in the crystal structures of DME polymorphs (a) β and (b) γ. The symmetry independent molecules are indicated in green, whereas the CH···O contacts are marked by dotted lines.

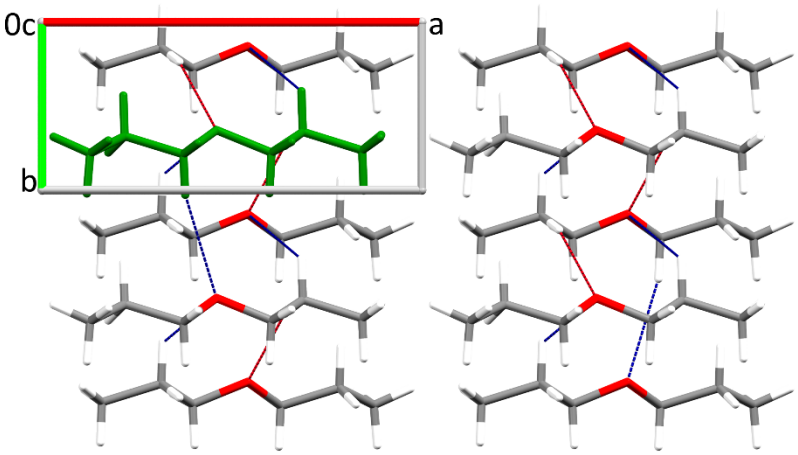


**Figure S26.** CH···O hydrogen bonding patterns in the high-pressure crystal structure of DPE. The symmetry independent molecule is indicated in green, whereas the CH···O contacts are marked by dotted lines.

**Table S1.** Crystal data and structure refinement details of DME phase β at 3.30, 3.90, 4.30 GPa and phase γ at 4.50, 5.60, 7.30 GPa (all at 295 K).

| | $C_2H_6O$ phase β | $C_2H_6O$ phase β | $C_2H_6O$ phase β | $C_2H_6O$ phase γ | $C_2H_6O$ phase γ | $C_2H_6O$ phase γ |
|---|---|---|---|---|---|---|
| Pressure (GPa) | 3.30(2) | 3.90(2) | 4.30(2) | 4.50(2) | 5.60(2) | 7.30(2) |
| Temperature (K) | 295(2) | 295(2) | 295(2) | 295(2) | 295(2) | 295(2) |
| Formula weight | 46.07 | 46.07 | 46.07 | 46.07 | 46.07 | 46.07 |
| Crystal colour | colourless | colourless | colourless | colourless | colourless | colourless |
| Crystal size (mm) | 0.30x0.29x0.25 | 0.33x0.33x0.24 | 0.38x0.38x0.23 | 0.34x0.32x0.22 | 0.37x0.35x0.21 | 0.40x0.38x0.20 |
| Crystal system | monoclinic | monoclinic | monoclinic | triclinic | triclinic | triclinic |
| Space group | $P2_1/c$ | $P2_1/c$ | $P2_1/c$ | $P\bar{1}$ | $P\bar{1}$ | $P\bar{1}$ |
| Unit cell dimensions | | | | | | |
| $a$ (Å) | 5.5541(4) | 5.5277(4) | 5.5073(4) | 4.3394(12) | 4.2888(17) | 4.250(4) |
| $b$ (Å) | 6.6179(11) | 6.527(10) | 6.493(5) | 8.414(2) | 8.3045(18) | 8.198(3) |
| $c$ (Å) | 6.964(3) | 6.8941(5) | 6.8431(8) | 12.821(6) | 12.7912(13) | 12.6105(19) |
| $\alpha$ (°) | 90 | 90 | 90 | 90.55(4) | 90.249(12) | 90.641(19) |
| $\beta$ (°) | 103.835(19) | 103.869(6) | 103.848(8) | 93.89(6) | 93.92(2) | 93.97(3) |
| $\gamma$ (°) | 90 | 90 | 90 | 90.83(2) | 90.14(3) | 90.04(5) |
| Volume (Å$^3$) | 248.56(12) | 241.5(4) | 237.58(19) | 467.0(3) | 454.5(2) | 438.3(4) |
| $Z$, $Z'$ | 4, 1 | 4, 1 | 4, 1 | 8, 4 | 8, 4 | 8, 4 |
| $V/Z$ | 62.14(3) | 60.375(1) | 59.395(5) | 58.375(4) | 56.8125(3) | 54.7875(5) |
| $D_x$ (g·cm$^{-3}$) | 1.231 | 1.267 | 1.288 | 1.311 | 1.346 | 1.396 |
| Wavelength MoKα, λ (Å) | 0.71073 | 0.71073 | 0.71073 | 0.71073 | 0.71073 | 0.71073 |
| Absorption coefficient (mm$^{-1}$) | 0.095 | 0.098 | 0.100 | 0.101 | 0.104 | 0.108 |
| $F$(000) (e) | 104 | 104 | 104 | 208 | 208 | 208 |
| 2Θ max (°) | 51.82 | 51.45 | 52.24 | 52.31 | 52.51 | 52.24 |
| Min./Max. indices $h$, $k$, $l$ | -6/6, -7/7, -4/4 | -6/6, -1/1, -8/8 | -6/6, -3/3, -7/7 | -5/5, -10/10, -5/6 | -2/2, -10/9, -15/15 | -2/2, -9/9, -15/15 |
| Reflections collected/unique | 850/147 | 634/107 | 721/129 | 2659/556 | 2631/559 | 2349/523 |
| $R_{int}$ (all data) | 0.0646 | 0.0308 | 0.0295 | 0.0338 | 0.0306 | 0.0418 |
| Observed reflections ($F^2 > 2\sigma(F^2)$) | 132 | 99 | 118 | 481 | 486 | 389 |
| Data/restraints/parameters | 147/0/31 | 107/0/15 | 129/0/31 | 556/0/117 | 559/0/58 | 523/0/118 |
| Goodness of fit on $F^2$ | 1.204 | 1.192 | 1.181 | 1.131 | 1.135 | 1.055 |
| Final $R_1$ indices ($F^2 > 2\sigma(F^2)$) | 0.0708 | 0.0690 | 0.0525 | 0.0554 | 0.1173 | 0.0793 |
| $R_1/wR_2$ indices (all data) | 0.0776/0.1927 | 0.0728/0.1724 | 0.0566/0.1399 | 0.0628/0.1553 | 0.1296/0.2604 | 0.1062/0.1868 |
| $\Delta\sigma_{max}$, $\Delta\sigma_{min}$ (eÅ$^{-3}$) | 0.19/-0.17 | 0.17/-0.12 | 0.14/-0.11 | 0.15/-0.14 | 0.23/-0.19 | 0.15/-0.14 |
| Weighting scheme: x; y[a] | 0.1102;0.24 | 0.1005/0.17 | 0.1045/0.04 | 0.0885/0.32 | 0.0699/2.71 | 0.0557/1.68 |

[a] $w=1/(\sigma^2(Fo^2)+x^2P^2+yP)$, where $P=(\mathrm{Max}(Fo^2,0)+2Fc^2)/3$

**Table S2.** Crystal data and structure refinement details of DEE phase β at 1.85, 2.15, 2.45, 2.65 GPa and phase γ at 2.65 GPa (all at 295 K).

| | $C_4H_{10}O$ phase β | $C_4H_{10}O$ phase β | $C_4H_{10}O$ phase β | $C_4H_{10}O$ phase β | $C_4H_{10}O$ phase γ |
|---|---|---|---|---|---|
| Pressure (GPa) | 1.85(2) | 2.15(2) | 2.45(2) | 2.65(2) | 2.65(2) |
| Temperature (K) | 295(2) | 295(2) | 295(2) | 295(2) | 295(2) |
| Formula weight | 74.12 | 74.12 | 74.12 | 74.12 | 74.12 |
| Crystal colour | colourless | colourless | colourless | colourless | colourless |
| Crystal size (mm) | 0.37x0.36x0.27 | 0.38x0.34x0.26 | 0.39x0.36x0.25 | 0.40x0.37x0.24 | 0.40x0.36x0.24 |
| Crystal system | monoclinic | monoclinic | monoclinic | monoclinic | monoclinic |
| Space group | $P2_1/c$ | $P2_1/c$ | $P2_1/c$ | $P2_1/c$ | $I2/a$ |
| Unit cell dimensions | | | | | |
| $a$ (Å) | 6.8268(3) | 6.7948(3) | 6.7759(3) | 6.7612(3) | 7.7073(12) |
| $b$ (Å) | 8.1428(17) | 8.0952(12) | 8.0552(14) | 8.0271(15) | 4.0885(4) |
| $c$ (Å) | 7.7731(3) | 7.7259(2) | 7.6873(2) | 7.6687(3) | 13.233(2) |
| $\beta$ (°) | 93.443(4) | 93.621(3) | 93.713(3) | 93.784(4) | 93.793(16) |
| Volume (Å$^3$) | 431.32(9) | 424.12(7) | 418.70(8) | 415.29(8) | 416.07(10) |
| $Z$, $Z'$ | 4, 1 | 4, 1 | 4, 1 | 4, 1 | 4, 0.5 |
| $V/Z$ | 107.83(2) | 106.03(2) | 104.675(2) | 103.8225(2) | 104.0175(3) |
| $D_x$ (g·cm$^{-3}$) | 1.141 | 1.161 | 1.176 | 1.185 | 1.183 |
| Wavelength MoKα, λ (Å) | 0.71073 | 0.71073 | 0.71073 | 0.71073 | 0.71073 |
| Absorption coefficient (mm$^{-1}$) | 0.079 | 0.080 | 0.081 | 0.082 | 0.081 |
| $F$(000) € | 168 | 168 | 168 | 168 | 168 |
| 2Θ max (°) | 52.79 | 53.27 | 52.89 | 52.79 | 52.71 |
| Min./Max. indices $h$, $k$, $l$ | -8/8, -5/5, -9/9 | -8/8, -5/5, -9/9 | -8/8, -5/5, -9/9 | -8/7, -5/5, -9/9 | -7/8, -4/4, -14/14 |
| Reflections collected/unique | 2198/386 | 2208/386 | 2154/377 | 2120/375 | 1160/223 |
| $R_{int}$ (all data) | 0.0239 | 0.0250 | 0.0245 | 0.0216 | 0.0131 |
| Observed reflections ($F^2 > 2\sigma(F^2)$) | 352 | 353 | 346 | 342 | 202 |
| Data/restraints/parameters | 386/0/48 | 386/0/48 | 377/0/48 | 375/0/48 | 223/0/25 |
| Goodness of fit on $F^2$ | 1.121 | 1.168 | 1.138 | 1.088 | 1.130 |
| Final $R_1$ indices ($F^2 > 2\sigma(F^2)$) | 0.0353 | 0.0327 | 0.0390 | 0.0388 | 0.0371 |
| $R_1/wR_2$ indices (all data) | 0.0403/0.0988 | 0.0367/0.0928 | 0.0421/0.1110 | 0.0423/0.1110 | 0.0417/0.1085 |
| $\Delta\sigma_{max}$, $\Delta\sigma_{min}$ (eÅ$^{-3}$) | 0.10/-0.11 | 0.09/-0.09 | 0.12/-0.12 | 0.14/-0.15 | 0.09/-0.11 |
| Weighting scheme: x; y[a] | 0.0644;0.04 | 0.0569/0.03 | 0.0773/0.03 | 0.0819/0.03 | 0.0545/0.17 |

[a] $w=1/(\sigma^2(Fo^2)+x^2P^2+yP)$, where $P=(\mathrm{Max}(Fo^2,0)+2Fc^2)/3$

**Table S3.** Crystal data and structure refinement details of DEE phase δ at 2.80, 3.45, 3.70, 4.90 GPa (all at 295 K).

| | **$C_4H_{10}O$ phase δ** | **$C_4H_{10}O$ phase δ** | **$C_4H_{10}O$ phase δ** | **$C_4H_{10}O$ phase δ** |
|---|---|---|---|---|
| Pressure (GPa) | 2.80(2) | 3.45(2) | 3.70(2) | 4.90(2) |
| Temperature (K) | 295(2) | 295(2) | 295(2) | 295(2) |
| Formula weight | 74.12 | 74.12 | 74.12 | 74.12 |
| Crystal colour | colourless | colourless | colourless | colourless |
| Crystal size (mm) | 0.36x0.36x0.23 | 0.37x0.37x0.22 | 0.38x0.38x0.21 | 0.40x0.40x0.20 |
| Crystal system | triclinic | triclinic | triclinic | triclinic |
| Space group | $P\bar{1}$ | $P\bar{1}$ | $P\bar{1}$ | $P\bar{1}$ |
| Unit cell dimensions | | | | |
| *a* (Å) | 5.1196(4) | 5.0809(5) | 5.072(3) | 5.0182(19) |
| *b* (Å) | 5.6659(10) | 5.6329(10) | 5.629(2) | 5.575(3) |
| *c* (Å) | 7.2999(4) | 7.2451(10) | 7.215(5) | 7.136(3) |
| *α* (°) | 97.275(8) | 97.382(13) | 97.43(5) | 97.36(4) |
| *β* (°) | 102.728(6) | 102.749(10) | 102.91(6) | 102.81(3) |
| *γ* (°) | 96.747(10) | 97.002(11) | 97.15(5) | 97.72(4) |
| Volume (Å$^3$) | 202.56(4) | 198.13(5) | 196.6(2) | 190.31(14) |
| *Z*, *Z'* | 2, 1 | 2, 1 | 2, 1 | 2, 1 |
| *V/Z* | 101.28(2) | 99.065(3) | 98.3(1) | 95.155(7) |
| $D_x$ (g·cm$^{-3}$) | 1.215 | 1.242 | 1.252 | 1.293 |
| Wavelength MoKα, λ (Å) | 0.71073 | 0.71073 | 0.71073 | 0.71073 |
| Absorption coefficient (mm$^{-1}$) | 0.084 | 0.086 | 0.086 | 0.089 |
| *F*(000) (e) | 84 | 84 | 84 | 84 |
| 2Θ max (°) | 52.25 | 52.25 | 55.46 | 55.72 |
| Min./Max. indices *h*, *k*, *l* | -6/6, -4/4, -8/8 | -6/6, -5/4, -8/8 | -5/5, -7/7, -7/7 | -5/5, -6/6, -8/8 |
| Reflections collected/unique | 1217/244 | 1179/243 | 1025/199 | 944/195 |
| $R_{int}$ (all data) | 0.0138 | 0.0183 | 0.0383 | 0.0950 |
| Observed reflections ($F^2 > 2\sigma(F^2)$) | 225 | 218 | 177 | 153 |
| Data/restraints/parameters | 244/0/48 | 243/0/23 | 199/0/23 | 195/0/23 |
| Goodness of fit on $F^2$ | 1.179 | 1.788 | 1.166 | 1.086 |
| Final $R_1$ indices ($F^2 > 2\sigma(F^2)$) | 0.0388 | 0.1011 | 0.0489 | 0.0610 |
| $R_1/wR_2$ indices (all data) | 0.0419/0.1000 | 0.1071/0.3608 | 0.0553/0.1407 | 0.0739/0.1816 |
| $\Delta\sigma_{max}$, $\Delta\sigma_{min}$ (eÅ$^{-3}$) | 0.09/-0.08 | 0.30/-0.29 | 0.09/-0.10 | 0.12/-0.12 |
| Weighting scheme: x; y[a] | 0.0403/0.09 | 0.2000/0 | 0.0907/0.03 | 0.1287/0.01 |

[a] $w=1/(\sigma^2(Fo^2)+x^2P^2+yP)$, where $P=(\mathrm{Max}(Fo^2,0)+2Fc^2)/3$

**Table S4.** Crystal data and structure refinement details of DPE phase α at 1.70, 2.10, 2.80, 3.85, 5.30 GPa (all at 295 K).

| | $C_6H_{14}O$ phase α | $C_6H_{14}O$ phase α | $C_6H_{14}O$ phase α | $C_6H_{14}O$ phase α | $C_6H_{14}O$ phase α |
|---|---|---|---|---|---|
| Pressure (GPa) | 1.70(2) | 2.10(2) | 2.80(2) | 3.85(2) | 5.30(2) |
| Temperature (K) | 295(2) | 295(2) | 295(2) | 295(2) | 295(2) |
| Formula weight | 102.18 | 102.18 | 102.18 | 102.18 | 102.18 |
| Crystal colour | colourless | colourless | colourless | colourless | colourless |
| Crystal size (mm) | 0.39x0.37x0.25 | 0.39x0.38x0.24 | 0.46x0.43x0.23 | 0.38x0.36x0.22 | 0.44x0.40x0.21 |
| Crystal system | monoclinic | monoclinic | monoclinic | monoclinic | monoclinic |
| Space group | $P2_1/c$ | $P2_1/c$ | $P2_1/c$ | $P2_1/c$ | $P2_1/c$ |
| Unit cell dimensions | | | | | |
| $a$ (Å) | 9.416(4) | 9.368(8) | 9.293(7) | 9.198(9) | 9.099(12) |
| $b$ (Å) | 4.1817(3) | 4.1229(4) | 4.0686(2) | 4.0064(3) | 3.9465(3) |
| $c$ (Å) | 15.579(7) | 15.434(4) | 15.1855(10) | 14.9459(15) | 14.649(8) |
| $\beta$ (°) | 101.23(5) | 100.84(6) | 100.35(3) | 99.54(4) | 98.32(10) |
| Volume (Å$^3$) | 601.7(4) | 585.5(6) | 564.8(4) | 543.1(5) | 520.5(7) |
| $Z$, $Z'$ | 4, 1 | 4, 1 | 4, 1 | 4, 1 | 4, 1 |
| $V/Z$ | 150.425(1) | 146.375(1) | 141.2(1) | 135.775(1) | 130.125(2) |
| $D_x$ (g·cm$^{-3}$) | 1.128 | 1.159 | 1.202 | 1.249 | 1.304 |
| Wavelength MoKα, λ (Å) | 0.71073 | 0.71073 | 0.71073 | 0.71073 | 0.71073 |
| Absorption coefficient (mm$^{-1}$) | 0.073 | 0.075 | 0.078 | 0.081 | 0.085 |
| $F$(000) (e) | 232 | 232 | 232 | 232 | 232 |
| 2Θ max (°) | 52.86 | 53.06 | 53.10 | 52.91 | 52.55 |
| Min./Max. indices $h$, $k$, $l$ | -8/8, -5/5, -14/14 | -6/6, -5/5, -16/16 | -4/4, -5/5, -19/19 | -4/4, -5/5, -18/18 | -7/7, -4/4, -16/16 |
| Reflections collected/unique | 3001/386 | 2850/383 | 2881/356 | 2785/347 | 2594/310 |
| $R_{int}$ (all data) | 0.0254 | 0.0297 | 0.0270 | 0.0297 | 0.0350 |
| Observed reflections ($F^2 > 2\sigma(F^2)$) | 286 | 287 | 282 | 281 | 232 |
| Data/restraints/parameters | 386/0/66 | 383/0/66 | 356/0/66 | 347/0/66 | 310/6/66 |
| Goodness of fit on $F^2$ | 1.077 | 1.053 | 1.082 | 1.111 | 1.060 |
| Final $R_1$ indices ($F^2 > 2\sigma(F^2)$) | 0.0455 | 0.0524 | 0.0456 | 0.0308 | 0.0469 |
| $R_1/wR_2$ indices (all data) | 0.0661/0.1513 | 0.0723/0.1416 | 0.0591/0.1447 | 0.0424/0.0900 | 0.0666/0.1229 |
| $\Delta\sigma_{max}$, $\Delta\sigma_{min}$ (eÅ$^{-3}$) | 0.10/-0.09 | 0.10/-0.10 | 0.09/-0.12 | 0.05/-0.06 | 0.10/-0.08 |
| Weighting scheme: x; y[a] | 0.1115/0.01 | 0.0676/0.31 | 0.0950/0.11 | 0.0571/0.02 | 0.0445/0.34 |

[a] $w=1/(\sigma^2(Fo^2)+x^2P^2+yP)$, where $P=(\mathrm{Max}(Fo^2,0)+2Fc^2)/3$